Charm, beauty and charmonium production at HERA–B

The HERA–B Collaboration

A. Zoccoli[6,a], I. Abt[23], M. Adams[10], M. Agari[13], H. Albrecht[12], A. Aleksandrov[29], V. Amaral[8], A. Amorim[8], S. J. Aplin[12], V. Aushev[16], Y. Bagaturia[12,36], V. Balagura[22], M. Bargiotti[6], O. Barsukova[11], J. Bastos[8], J. Batista[8], C. Bauer[13], Th. S. Bauer[1], A. Belkov[11,†], Ar. Belkov[11], I. Belotelov[11], A. Bertin[6], B. Bobchenko[22], M. Böcker[26], A. Bogatyrev[22], G. Bohm[29], M. Bräuer[13], M. Bruinsma[28,1], M. Bruschi[6], P. Buchholz[26], T. Buran[24], J. Carvalho[8], P. Conde[2,12], C. Cruse[10], M. Dam[9], K. M. Danielsen[24], M. Danilov[22], S. De Castro[6], H. Deppe[14], X. Dong[3], H. B. Dreis[14], V. Egorytchev[12], K. Ehret[10], F. Eisele[14], D. Emeliyanov[12], S. Essenov[22], L. Fabbri[6], P. Faccioli[6], M. Feuerstack-Raible[14], J. Flammer[12], B. Fominykh[22], M. Funcke[10], Ll. Garrido[2], B. Giacobbe[6], P. Giovannini[6], J. Gläß[20], D. Goloubkov[12,33], Y. Golubkov[12,34], A. Golutvin[22], I. Golutvin[11], I. Gorbounov[12,26], A. Gorišek[17], O. Gouchtchine[22], D. C. Goulart[7], S. Gradl[14], W. Gradl[14], F. Grimaldi[6], Yu. Guilitsky[22,35], J. D. Hansen[9], J. M. Hernández[29], W. Hofmann[13], T. Hott[14], W. Hulsbergen[1], U. Husemann[26], O. Igonkina[22], M. Ispiryan[15], T. Jagla[13], C. Jiang[3], H. Kapitza[12], S. Karabekyan[25], N. Karpenko[11], S. Keller[26], J. Kessler[14], F. Khasanov[22], Yu. Kiryushin[11], E. Klinkby[9], K. T. Knöpfle[13], H. Kolanoski[5], S. Korpar[21,17], C. Krauss[14], P. Kreuzer[12,19], P. Križan[18,17], D. Krücker[5], S. Kupper[17], T. Kvaratskheliia[22], A. Lanyov[11], K. Lau[15], B. Lewendel[12], T. Lohse[5], B. Lomonosov[12,32], R. Männer[20], S. Masciocchi[12], I. Massa[6], I. Matchikhilian[22], G. Medin[5], M. Medinnis[12], M. Mevius[12], A. Michetti[12], Yu. Mikhailov[22,35], R. Mizuk[22], R. Muresan[9], M. zur Nedden[5], M. Negodaev[12,32], M. Nörenberg[12], S. Nowak[29], M. T. Núñez Pardo de Vera[12], M. Ouchrif[28,1], F. Ould-Saada[24], D. Peralta[2], R. Pernack[25], R. Pestotnik[17], M. Piccinini[6], M. A. Pleier[13], M. Poli[6,31], V. Popov[22], D. Pose[11,14], S. Prystupa[16], V. Pugatch[16], Y. Pylypchenko[24], J. Pyrlik[15], K. Reeves[13], D. Reßing[12], H. Rick[14], I. Riu[12], P. Robmann[30], I. Rostovtseva[22], V. Rybnikov[12], F. Sánchez[13], A. Sbrizzi[1], M. Schmelling[13], B. Schmidt[12], A. Schreiner[29], H. Schröder[25], A. J. Schwartz[7], A. S. Schwarz[12], B. Schwenninger[10], B. Schwingenheuer[13], F. Sciacca[13], N. Semprini-Cesari[6], S. Shuvalov[22,5], L. Silva[8], L. Sözüer[12], S. Solunin[11], A. Somov[12], S. Somov[12,33], J. Spengler[13], R. Spighi[6], A. Spiridonov[29,22], A. Stanovnik[18,17], M. Starič[17], C. Stegmann[5], H. S. Subramania[15], M. Symalla[12,10], I. Tikhomirov[22], M. Titov[22], I. Tsakov[27], U. Uwer[14], C. van Eldik[12,10], Yu. Vassiliev[16], M. Villa[6], A. Vitale[6], I. Vukotic[5,29], H. Wahlberg[28], A. H. Walenta[26], M. Walter[29], J. J. Wang[4], D. Wegener[10], U. Werthenbach[26], H. Wolters[8], R. Wurth[12], A. Wurz[20], Yu. Zaitsev[22], M. Zavertyaev[12,13,32], G. Zech[26], T. Zeuner[12,26], A. Zhelezov[22], Z. Zheng[3], R. Zimmermann[25], T. Živko[17]

1 NIKHEF, 1009 DB Amsterdam, The Netherlands [a]
2 Department ECM, Faculty of Physics, University of Barcelona, E-08028 Barcelona, Spain [b]
3 Institute for High Energy Physics, Beijing 100039, P.R. China
  Institute of Engineering Physics, Tsinghua University, Beijing 100084, P.R. China
4 Institut für Physik, Humboldt-Universität zu Berlin, D-12489 Berlin, Germany [c,d]
5 Dipartimento di Fisica dell' Università di Bologna and INFN Sezione di Bologna, I-40126 Bologna, Italy
6 Department of Physics, University of Cincinnati, Cincinnati, Ohio 45221, USA [e]
7 LIP Coimbra, P-3004-516 Coimbra, Portugal [f]
8 Niels Bohr Institutet, DK 2100 Copenhagen, Denmark [g]
9 Institut für Physik, Universität Dortmund, D-44221 Dortmund, Germany [d]
10 Joint Institute for Nuclear Research Dubna, 141980 Dubna, Moscow region, Russia
11 DESY, D-22603 Hamburg, Germany
12 Max-Planck-Institut für Kernphysik, D-69117 Heidelberg, Germany [d]
13 Physikalisches Institut, Universität Heidelberg, D-69120 Heidelberg, Germany [d]
14 Department of Physics, University of Houston, Houston, TX 77204, USA [e]
15 Institute for Nuclear Research, Ukrainian Academy of Science, 03680 Kiev, Ukraine [h]
16 J. Stefan Institute, 1001 Ljubljana, Slovenia [i]
17 University of Ljubljana, 1001 Ljubljana, Slovenia
18 University of California, Los Angeles, CA 90024, USA [j]
19 Lehrstuhl für Informatik V, Universität Mannheim, D-68131 Mannheim, Germany
20 University of Maribor, 2000 Maribor, Slovenia
21 Institute of Theoretical and Experimental Physics, 117259 Moscow, Russia [k]

a e-mail: zoccoli@bo.infn.it

[22] Max-Planck-Institut für Physik, Werner-Heisenberg-Institut, D-80805 München, Germany [d]

[23] Dept. of Physics, University of Oslo, N-0316 Oslo, Norway [l]

[24] Fachbereich Physik, Universität Rostock, D-18051 Rostock, Germany [d]

[25] Fachbereich Physik, Universität Siegen, D-57068 Siegen, Germany [d]

[26] Institute for Nuclear Research, INRNE-BAS, Sofia, Bulgaria

[27] Universiteit Utrecht/NIKHEF, 3584 CB Utrecht, The Netherlands [a]

[28] DESY, D-15738 Zeuthen, Germany

[29] Physik-Institut, Universität Zürich, CH-8057 Zürich, Switzerland [m]

[30] visitor from Dipartimento di Energetica dell' Università di Firenze and INFN Sezione di Bologna, Italy

[31] visitor from P.N. Lebedev Physical Institute, 117924 Moscow B-333, Russia

[32] visitor from Moscow Physical Engineering Institute, 115409 Moscow, Russia

[33] visitor from Moscow State University, 119899 Moscow, Russia

[34] visitor from Institute for High Energy Physics, Protvino, Russia

[35] visitor from High Energy Physics Institute, 380086 Tbilisi, Georgia

Abstract. HERA–B is a fixed target experiment working on the 920 GeV proton beam of the HERA accelerator at the DESY laboratory in Hamburg. During the last data taking period (2002–2003), about 150 million dilepton triggers, 220 million minimum bias events and 35 million hard photon triggers were acquired. These large statistics allow detailed studies on the production of charmonium states in proton-nucleus p-A collisions, which extend for the first time into the negative Feynman-x (x_F) region. Measurements of the inclusive $b\bar{b}$, Υ and open charm cross sections are also ongoing. After a brief discussion of the detector and of the data samples, we report on preliminary results obtained on these physics topics.

PACS. 24.85.p, 13.85.Ni

1 Introduction

HERA–B is a fixed target experiment [1] working on the 920 GeV proton beam ($\sqrt{s} = 41.6$ GeV) of the HERA ring at DESY in Hamburg.

The physics program of the experiment covers a wide range of topics and is centered on the heavy flavor production. Other topics under investigation are strangeness and hyperon production, hard photon production, searches of exotic states (like pentaquarks, glueballs or hybrids), and the search of flavor-changing neutral currents (FCNC).

Emphasis is placed on the study of charmonium production (e.g. J/ψ, $\psi(2S)$ and χ_c) and its nuclear dependence in p-A collisions. For the first time it is possible to perform measurements in the negative x_F region. This will provide important tests for many different models attempting to describe the inclusive single-particle production and its modification in the nuclear matter. In this context the basic color singlet and color octet mechanisms [2] of quarkonium production are complemented with the inclusion of processes which try to account for the interaction with the nuclear matter, like the final state absorption, interactions with comovers, shadowing of parton distributions and parton energy loss [3]. The understanding of these particle production mechanisms will provide a solid baseline for the interpretation of the particle suppression studies in heavy-ion collisions, performed with the aim to observe quark-gluon-plasma formation.

HERA–B is also studying the production of b and c quarks in p-A collisions, by providing a new precise measurement of the $b\bar{b}$ cross section and of the Υ production, and by measuring the open charm cross section. This will provide important inputs and put further constraints on NLO QCD predictions.

In Sect. 2 we provide a short discussion of the detector and of trigger of the experiment, as well as a short
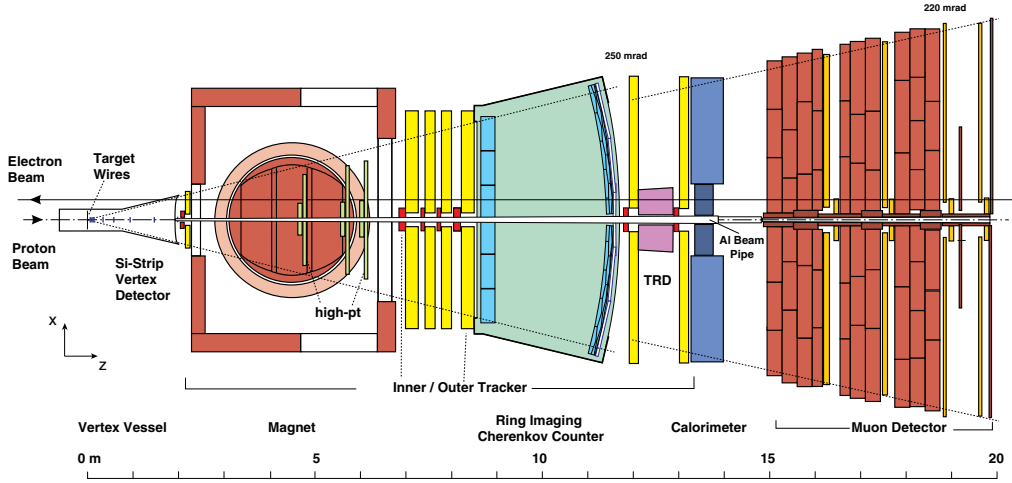
Fig. 1. Top view of the HERA–B detector

summary of the main data samples acquired. Section 4 describes the main preliminary results obtained on charmonium production. Sections 5 and 6 discuss the open charm production and the open and hidden beauty production. Finally the conclusions are drawn in Sect. 7.

2 The HERA–B detector

The HERA–B experiment is a forward magnetic spectrometer with an acceptance extending from 10 to 220 mrad horizontally and to 160 mrad vertically [1,4]. This large angular coverage allows us to study kinematic regions (like the negative x_F range for charmonium states) not accessible in previous high energy experiments. A top view of the detector is shown in Fig. 1. The first part of the spectrometer is devoted to tracking and vertex measurements and consists of a target, a silicon vertex detector, a magnet and a tracking system. The second part is focused on the particle identification and includes a Ring Imaging Cherenkov detector, an electromagnetic calorimeter and a muon detector.

The target system consists of two stations of 4 wires each, of different materials (C, Al, Pd, Ti, W), separated by 4 cm along the beam direction. It is placed in the halo of the HERA proton beam. The wire positions can be continuously adjusted in order to keep a constant interaction rate, in the range between 1 and 40 MHz. During the physics data taking only single-wire (mainly C or W) and double-wire (C and W) configurations were used, with a typical interaction rate of about 5 MHz.

The vertex detector (VDS) is placed between the target and the magnet and consists of 8 stations of double-sided silicon microstrip detectors (50×70 mm^2, 50 μm pitch). Each station consists of four "quadrants" arranged if four different stereo views. This system provides a primary vertex resolution of $\sigma_z \sim 500$ μm along the beam direction and $\sigma_{x,y} \sim 50$ μm in the transverse plane.

A dipole magnet with 2.13 Tm field-integral is positioned before the tracking system. Each tracking station consists of several planes of MSGC/GEM chambers

placed near the beam pipe (Inner Tracker, ITR) and several planes of Honeycomb Drift chambers which cover the rest of the acceptance (Outer Tracker, OTR). The detector segmentation is set in order to cope with the particle flux variation with the distance from the beam pipe. Typical momentum resolutions of $\sigma p/p \sim 1\%$ are achieved.

The particle identification for charged tracks (protons, kaons, etc.) is provided by a Cherenkov detector (RICH) installed downstream of the magnet. The electromagnetic calorimeter (ECAL), which provides the electron pretrigger seeds and the e/π separation, is installed after the RICH and the tracking system. The ECAL is a Shashlik sampling calorimeter with Pb or W as absorber and scintillator as active material. The Muon detector (MUON) provides the muon pretrigger seeds and the muon identification and is located in the most downstream part of the detector. It consists of four superlayers embedded in an iron loaded concrete absorber. The sensitive area close to the beam pipe is covered by pixel chambers, while in the rest of the acceptance tube chambers are used.

3 Trigger and data samples

The trigger is based on a multi-level scheme and has been designed to select with high efficiency the two leptons from the $J/\psi \to \ell^+\ell^-$ decay and to provide a large background suppression, reducing the initial interaction rate (~ 5 MHz) to the typical logging rate of ~ 100 Hz, without dead time. Pretrigger seeds from the ECAL or the MUON detectors are sent to the First Level Trigger (FLT). The FLT is a hardware tracking device based on Kalman filtering. It selects the lepton candidates with a maximum latency of 12 μs providing a rate reduction factor of ~ 250. The events accepted by the FLT are sent to the Second Level Trigger (SLT) which provides a refined track reconstruction including the VDS information. The SLT is implemented on a farm of 240 Linux-PCs and has a typical latency of 10 ms with another rate reduction factor of ~ 200. The full reconstruction of the events passing the trigger selection is performed online on a second farm of
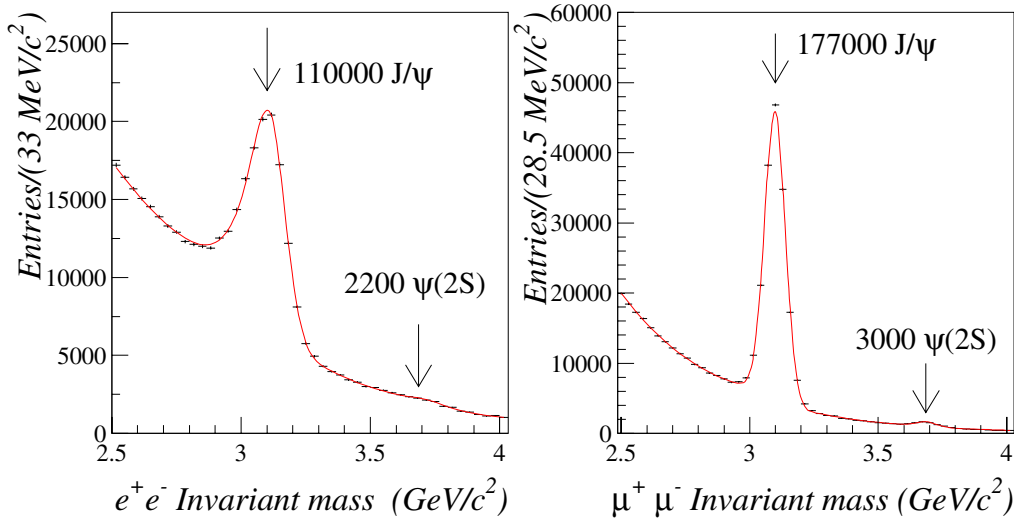
Fig. 2. e^+e^- (left) and $\mu^+\mu^-$ (right) invariant mass distributions in the region of the J/ψ and $\psi(2S)$ signals

about 200 Linux-PCs, providing a final logging rate on tape of ~ 100 Hz.

The scheme of this system allows to implement different trigger configurations, besides the main dilepton trigger. As a matter of fact, data have been taken requiring at least one energy deposit in ECAL with large transverse momentum (Hard Photon trigger). Another configuration required at least one inelastic interaction in the target (Minimum Bias trigger).

The data acquisition was performed in two different periods: a first short period, during the year 2000, mainly devoted to the debugging of the detector and of the trigger; a second longer period, from October 2002 to March 2003, for the physics program of the experiment.

The physics data taking has been performed by using three main different trigger configurations:

– Dilepton trigger. This trigger selects di-lepton events (e.g. e^+e^- or $\mu^+\mu^-$) with large transverse momentum. The total acquired statistics in this configuration is about 150 million of events, with an average DAQ rate of about 100 Hz.
– Minimum Bias (MB) trigger. This trigger requires at least one inelastic interaction in the target, by checking the presence of a minimum energy deposition in the RICH or in the ECAL detectors. The total collected statistics is about 220 million events, with an average DAQ rate larger than 1000 Hz.
– Hard photon trigger. It requires the presence in the ECAL of at least one cluster of high transverse energy (typically > 3 GeV). The total collected statistics corresponds to about 35 million events.

The results presented in this paper are derived from the first two trigger samples. The charmonium, the b-hadron and the Υ production studies are performed on the dilepton trigger sample, while the open charm cross section is measured in the MB sample.

4 Studies on charmonium production

The charmonium states are reconstructed exploiting their dilepton decay modes (e^+e^- and $\mu^+\mu^-$). The reconstruction requires the presence of two trigger tracks of opposite charge, with a common vertex and a good lepton identification. In the e^+e^- channel, where a large hadronic background is present, the electrons are identified by applying an E/p cut (where E is the electron energy measured by ECAL and p is its momentum measured by the tracking system), by performing a cluster shape analysis and by requiring a good match between the cluster in ECAL and the charged track. Moreover, possible energy losses due to the emission of a bremsstrahlung photon in the region before the magnet are taken into account. In the $\mu^+\mu^-$ channel, the request of a good muon likelihood is sufficient to strongly suppress the background.

Following these criteria about 300 000 J/ψ have been reconstructed in both decay channels. The corresponding invariant mass distributions are shown in Fig. 2. In the e^+e^- distribution a clear peak containing $\sim 110\,000$ J/ψ events is visible at the correct mass position [5], while in the muon channel the J/ψ peak contains $\sim 177\,000$ events. Also $\psi(2S)$ events have been reconstructed in the same invariant mass distributions, ~ 2200 in the e^+e^- channel and ~ 3000 in the $\mu^+\mu^-$ channel. In both channels the main contribution to the background is coming from pion and kaon decays, while physics processes like charm and beauty production give a small effect.
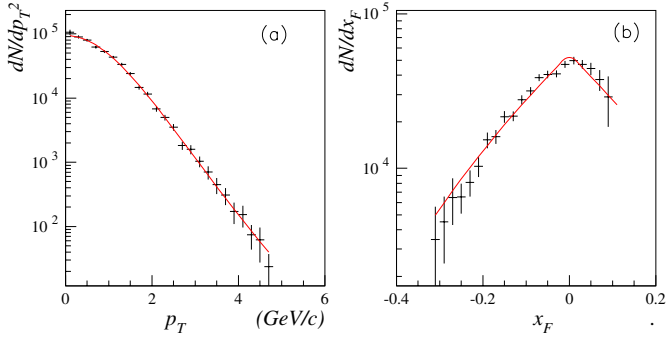
4.1 J/ψ differential distributions and nuclear dependence

These large statistics allowed detailed studies on the J/ψ p_T and x_F differential distributions and to measure the nuclear dependence of its production cross-section.

Figure 3 shows the preliminary results obtained on the electron channel for the p_T (a) and the x_F (b) differential

Table 1. Experimental situation on J/ψ differential distributions. The definition of the fitting parameters ($\langle p_T \rangle$ and c) is given in Eqs. 1 and 2. The kinematic intervals and the fitting parameters obtained from the e^+e^- channel of the HERA–B analysis are compared to fixed-target results at $\sqrt{s} = 38.8$ GeV [6]

Exp.	target (A)	p_T range (GeV/c)	$\langle p_T \rangle$ (GeV/c)	x_F range	c
HERA–B	C (12)	$0 \div 5.0$	1.22 ± 0.01	$-0.375 \div 0.125$	$5 \div 6.5$
	W (184)	$0 \div 5.0$	1.29 ± 0.01		$(\pm 0.2_{\text{stat}})$
E771	Si (28)	$0 \div 3.4$	1.20 ± 0.01	$-0.05 \div 0.25$	6.54 ± 0.23
E789	Be (9)			$0.30 \div 0.95$	5.32 ± 0.05
	Cu (64)			$0.30 \div 0.95$	5.21 ± 0.04
	Au (197)	$0 \div 2.6$	1.29 ± 0.01	$-0.035 \div 0.135$	4.91 ± 0.18
E672/E706	Be (9)	$0 \div 3.0$	1.22 ± 0.01	$0 \div 0.6$	6.18 ± 0.16

Fig. 3. J/ψ differential distributions, obtained in p-C collisions from the e^+e^- channel, as a function of p_T **a** and x_F **b**

Fig. 4. Nuclear suppression parameter, α, as a function of x_F (left) and p_T (right), as obtained from the full muon sample. Results from the E866 [7] (open circles) and NA50 [8] (open squares) experiments are also shown. The errors include statistical and systematic uncertainties

distributions, where the lines represent the fit results. The p_T and x_F distributions are fitted respectively with the functions:

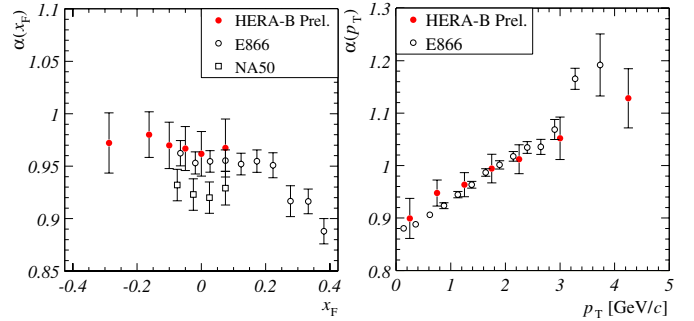$$\frac{\mathrm{d}N(J/\psi)}{\mathrm{d}p_T^2} = A \cdot \left[1 + \left(\frac{35 \cdot \pi \cdot p_T}{256 \cdot \langle p_T \rangle} \right)^2 \right]^{-6} \quad (1)$$

and

$$\frac{\mathrm{d}N(J/\psi)}{\mathrm{d}x_F} = B \cdot (1 - |x_F|)^c \quad (2)$$

where A and B are arbitrary normalization factors. The preliminary fit results on the average p_T and on the c exponent are reported in Tab. 1. As one can see, HERA–B extends significantly the p_T and x_F ranges for J/ψ's by accessing for the first time the negative x_F region. By comparing the results on the average p_T obtained from the p-C and the p-W data samples we confirm the tendency of an increase of the $\langle p_T \rangle$ with the mass number. The preliminary results on the x_F slopes are in the range 5–6.5 and the achievable final statistical accuracy is estimated to be ± 0.2.

The nuclear effects in heavy quark production are commonly parameterized by using the power law $\sigma_{pA} = \sigma_{pN} \cdot A^{\alpha(p_T, x_F)}$, where σ_{pA} is the production cross section in p-A collisions and σ_{pN} is the elementary proton-nucleon cross section. In order to measure the α exponent for the J/ψ production as a function of p_T and x_F only data taken

by using simultaneously the carbon and the tungsten targets have been used. This allowed to minimize the systematic effects depending on changes in the trigger and detector performances. Preliminary results obtained on the full muon sample are shown in Fig. 4 as a function of x_F and p_T. In the x_F range covered by HERA–B a small flat suppression is observed. The obtained average value of the nuclear suppression parameter α is:

$$\alpha = 0.969 \pm 0.003(\text{stat}) \pm 0.021(\text{syst}) \quad . \quad (3)$$

In the overlap region (i.e. for $x_F > -0.1$), our results are compatible with the E866 data [7] and are larger than the NA50 values [8]. Moreover, α increases with increasing p_T and, for large transverse momenta, an enhancement of J/ψ production ($\alpha > 1$) is observed. This is a consequence of the p_T broadening, in agreement with the observations of the E866 experiment [7]. This study is important for the verification of the different model predictions currently available for the nuclear suppression [9], and will be completed with the addition of the result from the e^+e^- channel.

Table 2. Preliminary results on the ratio $R(l^+l^-) = \mathcal{B}(\psi(2S) \to l^+l^-) \cdot \sigma(\psi(2S)) / \mathcal{B}(J/\psi \to l^+l^-) \cdot \sigma(J/\psi)$. The errors represent only the statistical uncertainties

Target	R(e^+e^-) (%)	R($\mu^+\mu^-$) (%)
Carbon	1.60 ± 0.20	1.65 ± 0.10
Tungsten	1.80 ± 0.40	1.55 ± 0.20

4.2 $\psi(2S)$ production

The comparison between $\psi(2S)$ and J/ψ production can further contribute to the understanding of nuclear absorption processes: different cross section behaviors of the two charmonium states, as a function of kinematic variables like x_F and p_T, may be interpreted in terms of the size and of the binding energy of these two charmonium states. Preliminary results on the total yield ratio $R(l^+l^-) = \mathcal{B}(\psi(2S) \to l^+l^-) \cdot \sigma(\psi(2S)) / \mathcal{B}(J/\psi \to l^+l^-) \cdot \sigma(J/\psi)$ have been obtained both from the e^+e^- and the $\mu^+\mu^-$ samples and are summarized in Table 2. These values confirm the apparent independence of the ratio R from the target mass number. Moreover, these results are in agreement with the world average result and show no dependence of R on the center of mass energy.

4.3 χ_c production

An additional check of the hadronic charmonium production models can be provided by the measurement of the fraction (R_{χ_c}) of J/ψ produced via the χ_c radiative decay $\chi_c \to $ J/$\psi\gamma$. Out of the three χ_c states, the χ_{c0} contribution is negligible, due to its small branching ratio [5], while the χ_{c1} and χ_{c2} states, separated by 46 MeV/c^2, cannot be resolved due to the insufficient energy resolution of the ECAL. For these reasons the ratio is quoted as:

$$R_{\chi_c} = \frac{\Sigma_{i=1}^2 \sigma(\chi_{ci})\mathcal{B}(\chi_{ci} \to J/\psi\gamma)}{\sigma(J/\psi)} \qquad (4)$$

where $\sigma(J/\psi)$ and $\sigma(\chi_{ci})$ are respectively the total production cross section of the J/ψ and of the χ_c states.

Figure 5 shows the $\Delta M = M(J/\psi\,\gamma) - M(J/\psi)$ distribution, referring to 15% of the total muon data sample, before (left) and after (right) the subtraction of the background. The main contributions to the background are the random combinations of J/ψ and photon candidates, and decays of heavier mesons into J/ψX. After background subtraction, we see a clear peak, corresponding to the two χ_c states, containing about 1300 events. The preliminary result, from this sub-sample of events, is:

$$R_{\chi_c} = 0.21 \pm 0.05_{stat} \qquad , \qquad (5)$$

where the error includes only statistical uncertainties. This result is in agreement with the previous HERA–B result $R_{\chi_c} = 0.32 \pm 0.06(\text{stat}) \pm 0.04(\text{syst})$. Moreover, it seems to favor the NRQCD predictions [2], even if a better

Table 3. Preliminary results obtained on D^0, D^+ and D^{*+} production cross sections (µb/nucl) and cross section ratios. The results are obtained from the full MB data sample, by summing up the data samples taken with different target materials. The second column gives the cross section in the HERA–B kinematic range, the third one gives the cross sections extrapolated to the full phase space using Pythia. The first error is due to statistics, the second to systematic uncertainties

Channel	Cross section $-0.1 < x_F < 0.05$	Cross section Full x_F range
σ_{D^0}	$21.4 \pm 3.2 \pm 3.6$	$56.3 \pm 8.5 \pm 9.5$
σ_{D^+}	$11.5 \pm 1.7 \pm 2.2$	$30.2 \pm 4.5 \pm 5.8$
$\sigma_{D^{*+}}$	$10.0 \pm 1.9 \pm 1.4$	$27.8 \pm 5.2 \pm 3.9$
$\sigma_{D^+}/\sigma_{D^0}$		$0.54 \pm 0.11 \pm 0.14$
$\sigma_{D^{*+}}/\sigma_{D^0}$		$0.49 \pm 0.12 \pm 0.10$

precision is needed to draw final conclusions. The number of χ_c expected in the full data sample is $\sim 15\,000$ which means an increase in statistics of about a factor 20 with respect to this analysis [10].

5 Open charm production

Signals of $D^0 \to K^-\pi^+$, $D^+ \to K^-\pi^+\pi^+$ and $D^{\star+} \to D^0\pi^+$ (and charge conjugate decays) are obtained from the minimum bias data sample. The HERA–B acceptance is limited to the mid-rapidity range, $x_F \in [-0.1, 0.05]$, while the p_T acceptance covers the range $p_T \in [0.0, 2.5]$ GeV/c. The D mesons are reconstructed requiring a good particle identification for the kaons and pions produced in the decay. Moreover the D-meson vertex is required to be separated from the primary one with high significance and the prolonged D-meson track must pass through the primary vertex. In this way it has been possible to reconstruct 189 ± 20 D^0, 198 ± 12 D^+ and 43 ± 8 $D^{\star+}$.

The corresponding production cross sections have been determined following the expression

$$\sigma_D = \frac{N_D}{\epsilon \cdot \mathcal{B} \cdot \Sigma A_i L_i} \qquad , \qquad (6)$$

where N_D is the number of reconstructed mesons, ϵ is the reconstruction efficiency, $\mathcal{B}$ is the corresponding branching ratio and $\mathcal{L} = \Sigma A_i L_i$ is the sum of the integrated luminosities over different target materials. The integrated luminosities have been measured by the ratio of the number of inelastic interactions (N_{inel}) recorded during the data taking period and the A-dependent inelastic cross section. N_{inel} has been determined in different ways: by looking at the signals of plastic scintillators placed behind the magnet, by measuring the total energy deposition in the ECAL, or from the probability to observe an empty event in a given subdetector [11]. The obtained preliminary results, summarized in Table 3, can be used to check the predictions of different QCD models [12] and to compare with previous experiments.
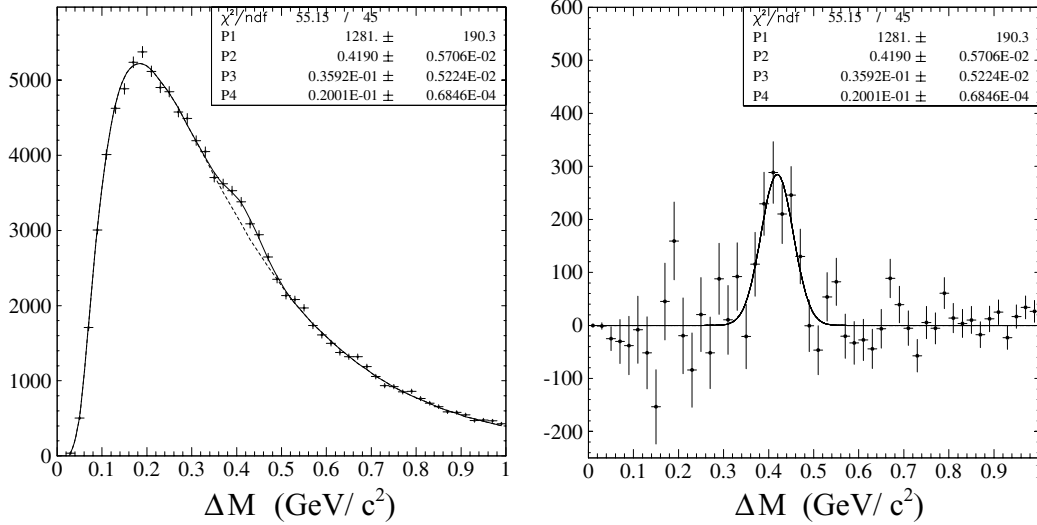
Fig. 5. χ_c signals in the $\Delta M = M(\text{J}/\psi\gamma) - M(\text{J}/\psi)$ invariant mass distribution, before (left) and after (right) background subtraction
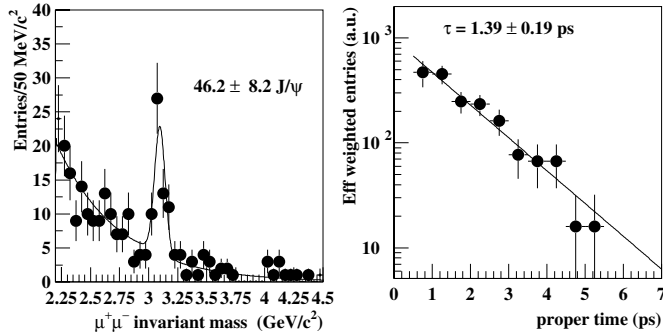
Fig. 6. Left: Dilepton mass for detached events from the full muon data sample. A J/ψ signal of about 50 events is clearly visible. Right: proper time distribution for the detached events sitting in the J/ψ mass region. The line represents the result of an unbinned likelihood fit of the events

6 Open and hidden beauty production

The open beauty production cross section, $\sigma(b\bar{b})$, is measured in the inclusive decay channel $B \to \text{J}/\psi X$, by looking at the $\text{J}/\psi \to l^+l^-$ decay modes. The $B \to \text{J}/\psi X$ events are selected by requiring J/ψ's detached with respect to the primary interaction vertex, exploiting the long lifetime of B-mesons. Moreover, both leptons have to be inconsistent with being produced in the primary interaction, by having large impact parameters to the target. In Fig. 6 (left) the mass of the selected dimuon candidates with a vertex downstream of the target, from the full data sample, is shown. A clear J/ψ peak of about 50 events is visible over a smooth background, which is mainly composed of π and K decays, and $b\bar{b}$ double semileptonic decay events. The right part of the figure shows the distribution of proper time for the detached J/ψ's, corrected for the selection efficiency. The line represents the result of an unbinned likelihood fit, which gives a lifetime of

$\tau = 1.39 \pm 0.19$ ps, well in agreement with the expected value for B-meson decays [5].

Combining the results in the e^+e^- and $\mu^+\mu^-$ channels, we obtain the following preliminary value for the cross section ratio in the HERA–B acceptance:

$$R_{\Delta\sigma} = \frac{\Delta\sigma(b\bar{b})}{\Delta\sigma(\text{J}/\psi)} = 0.033 \pm 0.005(\text{stat}) \pm 0.004(\text{syst}) . \quad (7)$$

Here, $\Delta\sigma$ represents the cross section in the HERA–B acceptance. In order to compare this result to other measurements and to theoretical predictions [13], we extrapolate the $R_{\Delta\sigma}$ ratio to the full x_{F} range and then, by using the prompt J/ψ cross section value $\sigma(\text{J}/\psi) = 357 \pm 2 \pm 36$ nb/nucl [14], we obtain the preliminary value for the total $b\bar{b}$ production cross section:

$$\sigma(b\bar{b}) = (9.9 \pm 1.5 \pm 1.4) \text{ nb/nucl} . \quad (8)$$

The statistics of $b\bar{b}$ events largely superseeds that of all earlier fixed target experiments. The result is within 2 standard deviations compatible with the previous HERA–B result [14].

In the high part of the dilepton mass spectra clear signals corresponding to the Υ states are observed. This allowed to perform a preliminary measurement of the Υ cross section, $\sigma(\Upsilon)$, times the branching ratio $Br(\Upsilon \to l^+l^-)$ at mid-rapidity. The preliminary combined e^+e^- $\mu^+\mu^-$ result yields:

$$\frac{d\sigma(\Upsilon)}{dy}\Big|_{y=0} \cdot Br(\Upsilon \to l^+l^-) = (3.4 \pm 0.8) \text{ pb/nucl} \quad , \quad (9)$$

with an uncertainty comparable or better than that of earlier experiments. Again, this result can be used to check and constrain the prediction of QCD models.

7 Conclusions

A brief overview on the studies performed by the HERA–B experiment in the field on heavy flavor production in p-A interactions has been given here. In most of the cases the presented results improve significantly the precision of previous measurements and provide useful input for QCD models and reference measurements for heavy-ion experiments.

References

1. E. Hartouni et al., An Experiment to Study CP Violation in the B System Using an Internal Target at the HERA Proton Ring Design Report, DESY-PRC 95/01 (1995)
2. P. Cho, A. Leibovich, Phys. Rev. D **53**, 150 (1996); M. Beneke, I.Z. Rothstein, Phys. Rev. D **54**, 2005 (1996); D **54**, 7082(E) (1996)
3. R. Vogt, Phys. Rev. C **61**, 035203 (2000)
4. The HERA–B Collaboration, Report on Status and prospects, DESY-PRC 00/04 (October 2000)
5. The Particle Data Group, Phys. Lett. B **592**, 1 (2004)
6. E789: M.S. Kowitt et al., Phys. Rev. Lett. **72**, 1318 (1994); M.H. Schub et al., Phys. Rev. D **52**, 1307 (1995) E771: T. Alexopoulos et al., Phys. Rev. D **55**, 3927 (1997): E672/E706: A. Gribushin et al., Phys. Rev. D **62**, 012001 (2000)
7. M. J. Leitch et al., Phys. Rev. Lett. **84**, 3256 (2000)
8. B. Alessandro et al., Eur. Phys. J. C **33**, 31 (2004)
9. R. Vogt, Nucl. Phys. A **700**, 539 (2002); K.G. Boreskov and A.B. Kaidalov, JETP Lett. **77**, 599 (2003)
10. HERA-B Collaboration, I. Abt et al., Phys. Lett. B **561**, 61 (2003)
11. HERA-B Collaboration, I. Abt et al., Eur. Phys. J. C **29**, 181 (2003)
12. N. Kidonakis et al., Phys. Rev. D **67**, 074037 (2003); R. Vogt, LBNL-report 49629 (2002), hep-ph/0203151
13. R. Bonciani et al., Nucl. Phys. B **529**, 424 (1998); N. Kidonakis et al., Eur. Phys. J. C **36**, 201 (2004)
14. HERA-B Collaboration, I. Abt et al., Eur. Phys. J. C **26**, 345 (2003)